MINISTRY OF EDUCATION AND TRAINING

VIET NAM ACADEMY OF SCIENCE AND TECHNOLOGY

GRADUATE UNIVERSITY OF SCIENCE AND TECHNOLOGY



PHAM MINH THUY

RESEARCH ON FABRICATION OF PHOTOCATALYTIC MATERIALS BASED ON TiO₂ AND ZnO MODIFIED BY NITROGEN-DOPED GRAPHENE QUANTUM DOTS AND SILVER NANOPARTICLES

SUMMARY OF DISSERTATION ON MATERIALS SCIENCE

Major: Theoretical and Physical Chemistry

Code: 9 44 01 19

The dissertation was completed at: Graduate University of Science and Technology, Vietnam Academy Science and Technology

Supervisors:

- 1. Supervisor 1: Assoc. Prof. Vu Duc Chinh, Institute of Institute of Materials Science, Vietnam Academy of Science and Technology
- 2. Supervisor 2: Dr. Chu Thi Thu Hien, Hanoi university of Civil Engineering

Refferee 1: Assoc. Prof. Nguyen Minh Phuong

Refferee 2: Assoc. Prof. Nguyen Manh Tuong

Refferee 3: Prof. Chu Manh Hoang

The dissertation is examined by Examination Board of Graduate University of Science and Technology, Vietnam Academy of Science and Technology at 9 AM, 24th September, 2025

The dissertation can be found at:

- 1. Graduate University of Science and Technology Library
- 2. National Library of Viet Nam

INTRODUCTION

The urgency of the thesis

Aquatic pollution caused by toxic organic substances in Vietnam, which are difficult to decompose, has been a rising problem in recent years. Combining noble metals and carbon nanomaterials with traditional photocatalysts can increase the decomposing yield of pollutants and enlarge the light absorption band. Therefore, natural sunlight can indeed be utilized to activate these materials, reducing the time and operating costs associated with the pollution treatment process.

Research objectives

- Synthesis of nitrogen-doped graphene quantum dots and silver nanoparticles modified TiO₂ and ZnO.
- Evaluate the photocatalytic activity of synthetic materials for methylene blue degradation in aquatic environments under light irradiation.

Research contents.

- + Research on the fabrication of TiO₂ and ZnO.
- + This research focuses on the fabrication of TiO₂ and ZnO materials that have been modified with silver (Ag) nanoparticles.
- + Research on the fabrication of TiO_2 and ZnO modified by nitrogendoped graphene quantum dots (N-GQDs).
- + Research on the fabrication of TiO_2 and ZnO materials modified with both N-GQDs and Ag nanoparticles.
 - + Investigate the characteristic properties of the fabricated materials.
- + Comparison of the photocatalytic capabilities of the synthesized materials.

Scientific and practical basis of the topic

Scientific basis

Ag nanomaterials have a lower Fermi energy than the conduction band energy of TiO₂, and ZnO serves as an electron trap. Additionally, N-GQDs

are novel semiconducting carbon materials with a narrow bandgap energy. When combined with photocatalytic materials, they can effectively utilize solar radiation in the visible spectrum. The integration of N-GQDs with precious metals like Ag and semiconducting oxides such as TiO_2 or ZnO holds the potential for producing unique scientific results.

Practical basis

The thesis presents initial experimental solutions and applications for the photocatalytic material systems Ag, N-GQDs/TiO₂ and Ag, N-GQDs/ZnO, aimed at decomposing well-dispersed organic compounds in an aqueous environment.

New contributions of the thesis

Science and Technology:

- The establishment of an environmentally friendly fabrication process for two new multilayer photocatalytic materials that effectively operate in the visible spectrum: Ag, N-GQDs/TiO₂ and Ag, N-GQDs/ZnO.
- An analysis of the optimal content ratio of nano silver and nitrogendoped graphene quantum dots that can be effectively modified on the surfaces of the traditional photocatalysts, titanium dioxide (TiO₂) and zinc oxide (ZnO).
- A proposal of a chemical structure model for N-GQDs, along with diagrams illustrating the reduction of Ag^+ ions to Ag by N-GQDs and charge transport in Ag, N-GQDs/TiO₂.
- A detailed outline of the processes involved in the emission and nonemission relaxation of electron-hole pairs in Ag/TiO₂ nanoparticles, including an analysis of the kinetics and insights into the decay processes.

Application:

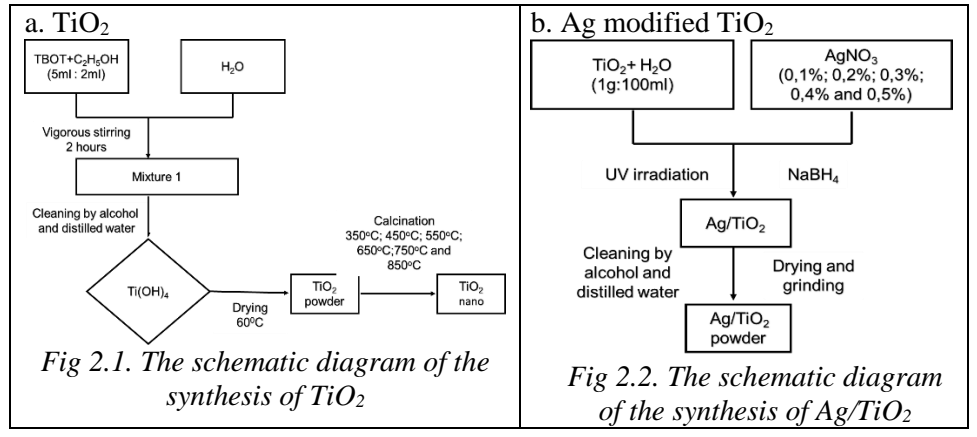
A viable technological solution for caffeine treatment has been proposed.

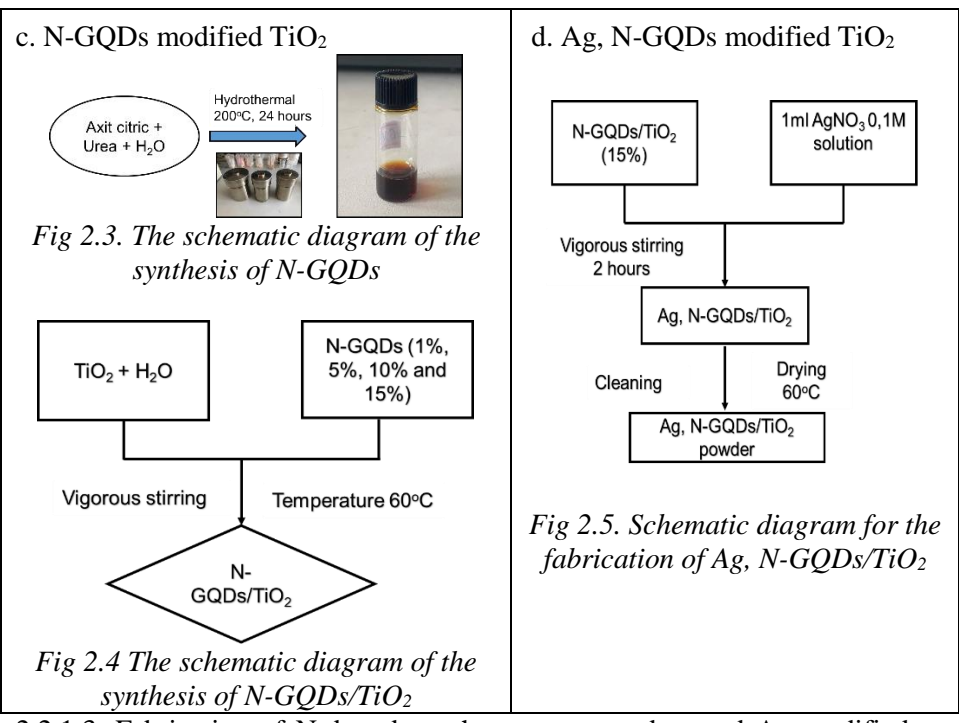
CHAPTER 1. LITERATURE REVIEW

- 1.1. Overview of Photocatalytic Materials
- 1.1.1. Mechanism of Photocatalytic Reactions
- 1.1.2. Factors Affecting Photocatalytic Activity
- 1.1.3. Titanium Dioxide
- 1.1.4. Zinc Oxide
- 1.2. Noble Metals
- 1.2.1. Mechanism of Charge Transport
- 1.2.2. Mechanism of Local Electric Field Enhancement
- 1.3. Graphene and Graphene Quantum Dots
- 1.3.1. Graphene
- 1.3.2. Graphene Quantum Dots
- 1.3.3. Mechanism of Enhanced Photocatalytic Efficiency in Graphene Materials
- 1.4. Current Research on Graphene and Noble Metals in Photocatalysis
- 1.5. Conclusion

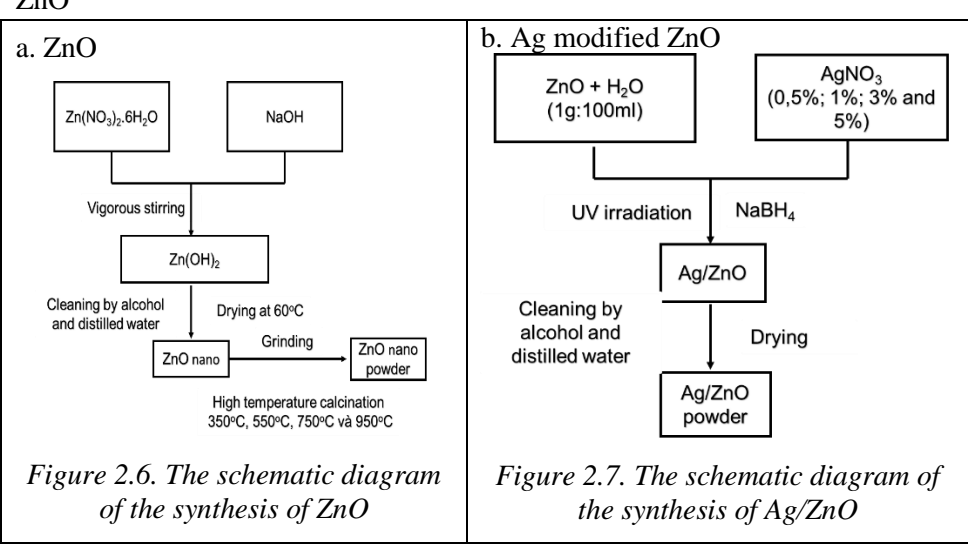
CHAPTER 2. OBJECTS AND RESEARCH METHODOLOGY

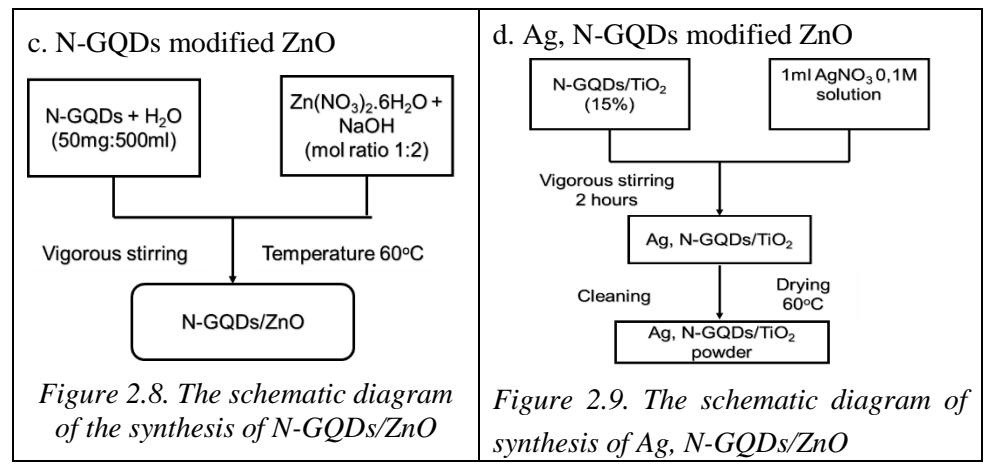
- 2.1. Research Objects
- 2.2. Research Methods
- 2.2.1. Synthesis Methods
- 2.2.1.2. Fabrication of N-doped graphene quantum dots and Ag nanoparticles modified ${\rm TiO_2}$





2.2.1.3. Fabrication of N-doped graphene quantum dots and Ag modified ZnO





2.2.2. Methods for Studying the Morphology and Structure of Materials

- 2.2.2.1. X-ray Diffraction
- 2.2.2.2. Scanning Electron Microscopy SEM
- 2.2.2.3. High-Resolution Transmission Electron Microscopy HRTEM
- 2.2.2.4. Fourier Transform Infrared Spectroscopy
- 2.2.2.5. X-ray Energy Dispersive Spectroscopy
- 2.2.2.6. X-Ray Photoelectron Spectroscopy
- 2.2.2.7. PL Fluorescence Spectroscopy
- 2.2.2.8. Raman Spectroscopy
- 2.2.2.9. UV-Vis Absorption Spectroscopy

2.2.3. Methods for Studying the Photocatalytic Activity of Materials

CHAPTER 3. RESEARCH RESULTS

3.1. Research results on the characteristics and photocatalytic activity of nitrogen-doped graphene quantum dots and silver-modified TiO₂.

3.1.1. Titanium Dioxide

- 3.1.1.1. Characteristics of TiO₂
- *a) X-ray diffraction pattern of TiO*₂

When the calcination temperature ranges from 350°C to 850°C, a phase transition of TiO₂ occurs. The form in which TiO₂ exists is temperature-

dependent; the anatase phase is present at temperatures below 650° C, while the rutile phase appears at temperatures above 650° C. This phase transition of TiO_2 is an irreversible process, and the crystal size of TiO_2 increases from 16 nm to 40 nm as the temperature rises.

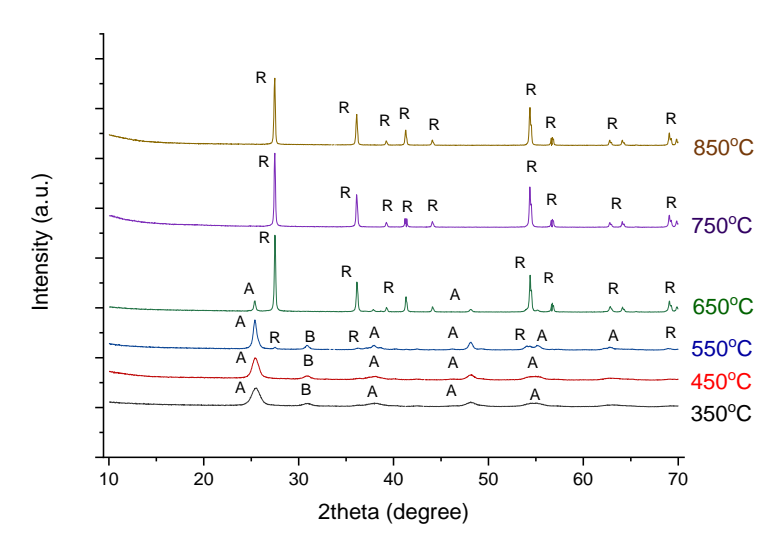


Figure 3.1. XRD pattern of TiO₂ synthesized using the sol-gel method and calcined at various temperatures.

Table 3.2. Crystal lattice parameters of TiO_2 material obtained from the XRD pattern.

Parameter	350°C	450°C	550°C	650°C	750°C	850°C
Crystal Phase	Brookite, Anatase	Brookite, Anatase	Brookite, Anatase, rutile	Anatase, Rutile	Rutie	Rutile
2θ (degree)	25.502	25.502	25.502	27.644	27.644	27.644
FWHM (radian)	1.04	0.811	0.47	0.18	0.17	0.16
Particle size (nm)	15.68	20.1	34.69	90.97	96.32	136.46
(hkl)	101	101	101	110	110	110

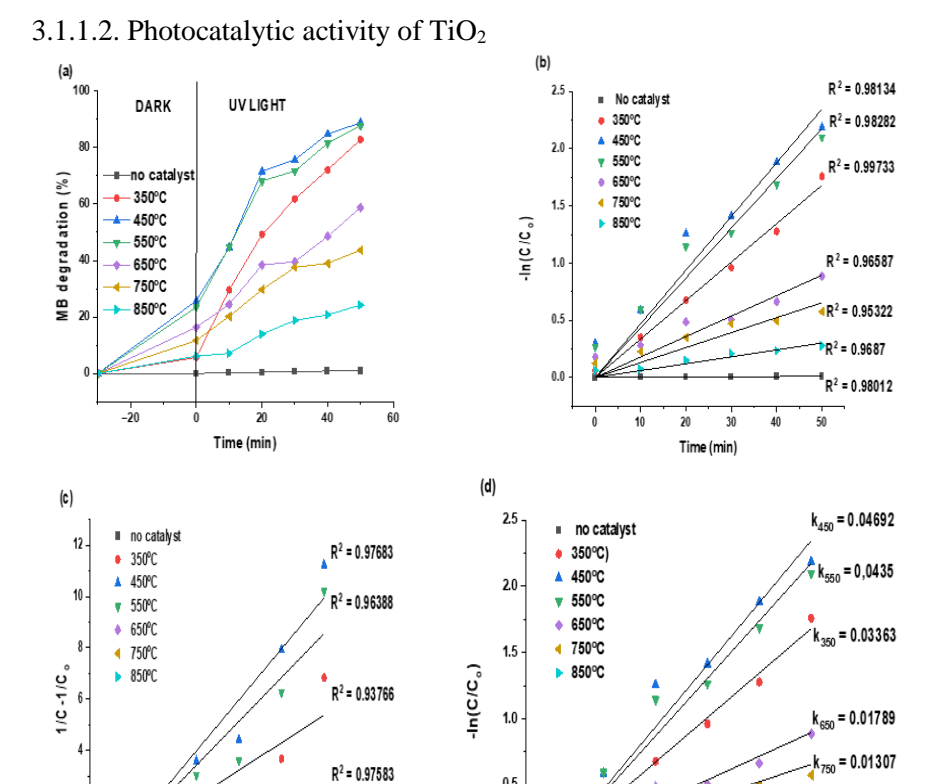


Figure 3.7. (a) Degradation efficiency, (b) first-order kinetic R^2 correlation coefficient, (c) second-order kinetic R^2 correlation coefficient, and (d) reaction rate constant values of the MB degradation process

 $R^2 = 0.9759$

 $R^2 = 0.98024$

0.5

0.0

k₈₅₀ = 0.00602

= 1.999 x10⁻⁴

40 50

Time (min)

2

10

30 20

Time (min)

All synthesized TiO₂ can effectively degrade organic dyes when exposed to UV light. TiO₂ that has been calcined at 450 °C shows the highest photocatalytic activity in the UV region. This material is capable of decomposing methylene blue (MB) and rhodamine B (RhB) with rate constants of $k = 0.04692 \text{ min}^{-1}$ (for MB) and $k = 0.0139 \text{ min}^{-1}$ (for RhB),

respectively. The synthesized TiO₂ exhibits greater efficiency in catalyzing the degradation of MB compared to RhB.

3.1.2. Ag modified TiO₂

c) Selected area electron diffraction (SAED) and high-resolution transmission electron microscopy (HRTEM) of Ag modified TiO₂ materials

Silver nanoparticles were uniformly distributed on the surface of TiO₂. The lattice distance of TiO₂ is 0.35 nm, while that of silver is 0.23 nm.

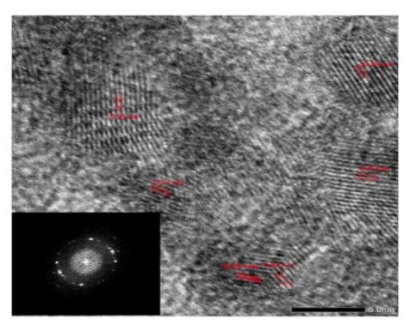
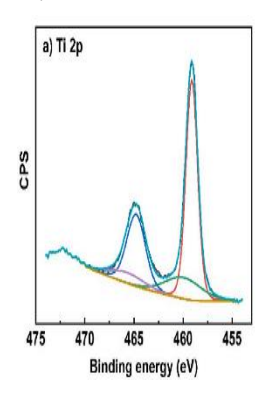
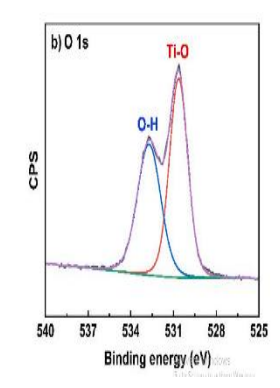


Figure 3.11. HRTEM images at high magnification of Ag/TiO₂

d) X-ray photoelectron spectrum (XPS) of Ag-modified TiO_2 material

The energy difference between the $Ti^{4+}2p_{1/2}$ and $Ti^{4+}2p_{3/2}$ states is 5.75 eV, which is consistent with the standard binding energy of TiO_2 . The high-resolution XPS spectra of Ag show two distinct peaks: Ag $3d_{5/2}$ at 368.4 eV and Ag $3d_{3/2}$ at 374.4 eV. This indicates that silver exists in its metallic form.





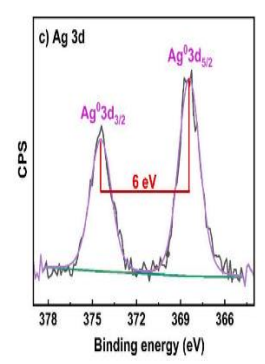


Figure 3.12. High resolution (a) Ti 2p, (b) O 1s and (c) Ag 3d XPS spectra of Ag/TiO₂

e) Photoluminescence spectra of Ag modified TiO₂

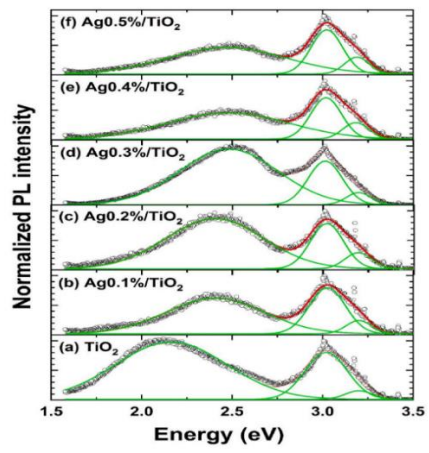


Figure 3.13. PL spectra of (a)TiO₂, (b)Ag0.1%/TiO₂, (c)Ag0.2%/TiO₂, (d)Ag0.3%/TiO₂, (e) Ag0.4%/TiO₂ and (f) Ag0.5%/TiO₂. The open circles and the lines are the experimental observations and the Gaussian fitted emission spectra, respectively

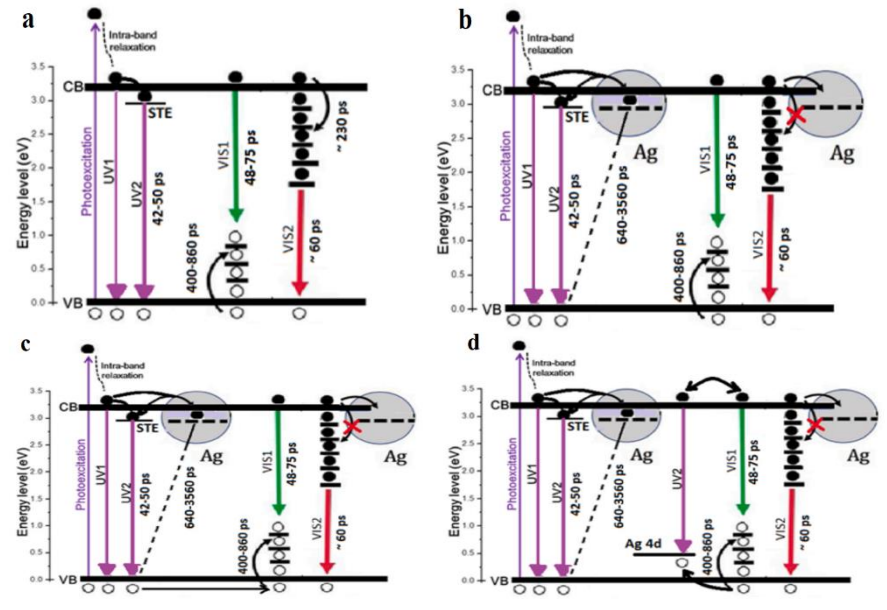
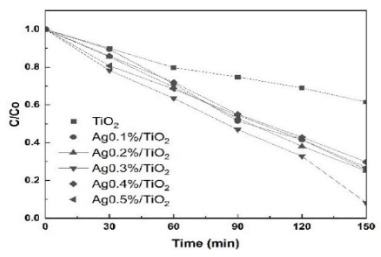


Figure 3.17. Schematic diagram of the decay pathways that are available upon photoexitation to the different populations of (a) TiO₂, (b) Ag0.1%-0.2%/TiO₂, (c) Ag0.3%/TiO₂, (d) Ag0.4 %-0.5% TiO₂

3.1.2.2. Photocatalytic activity of Ag modified TiO₂

 TiO_2 , when modified with silver at weights ranging from 0.1% to 0.5%, exhibits improved photocatalytic efficiency in the UV region compared to pure TiO_2 . Among these modifications, the sample with 0.3% Ag/TiO_2 demonstrates the highest photocatalytic efficiency. Consequently, this specific Ag weight content was chosen for further modification processes.



0.000 - 0.000

Figure 3.19. MB degradation efficiency of TiO₂ and Ag/TiO₂

Figure 3.20. Rate constant of MB degradation reaction of TiO_2 and Ag/TiO_2

3.1.3. N-doped graphene quantum dots and silver modified TiO₂

3.1.3.1. Characteristics of N-GQDs modified TiO_2

a) XRD pattern of N-GQDs modified TiO_2

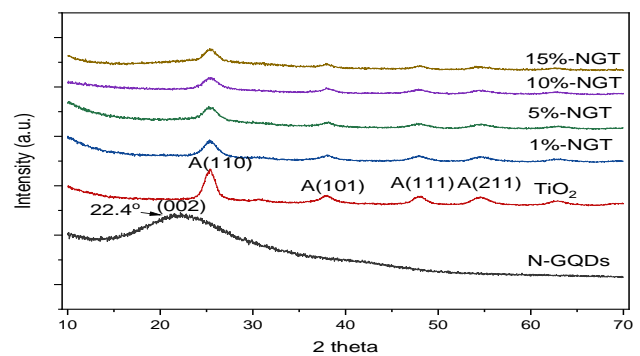
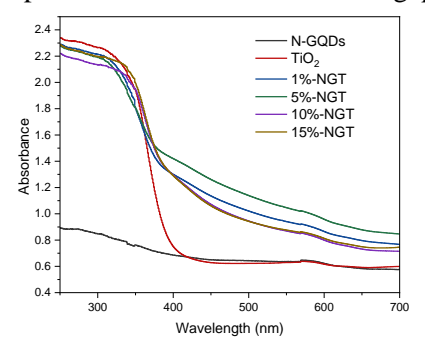


Figure 3.21. XRD pattern of TiO₂ and N-GQDs/TiO₂ c) UV-Vis spectra of N-GQDs modified TiO₂

The band gap energy of TiO_2 decreases when it is combined with N-GQDs materials, resulting in a red shift of the light absorption edge of these hybrid materials toward longer wavelengths. The N-GQDs $5\%/TiO_2$ composite exhibits the lowest band gap at 3.02 eV.



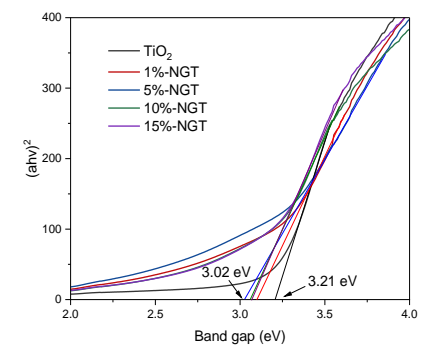


Figure 3.23. UV-Vis spectra of N-GQDs, pure TiO₂ and N-GQDs/TiO₂

Figure 3.24. Tauc plot and band gap of TiO₂ and N-GQDs/TiO₂

e) High-Resolution Transmission Electron Microscopy of N-GQDs modified TiO₂

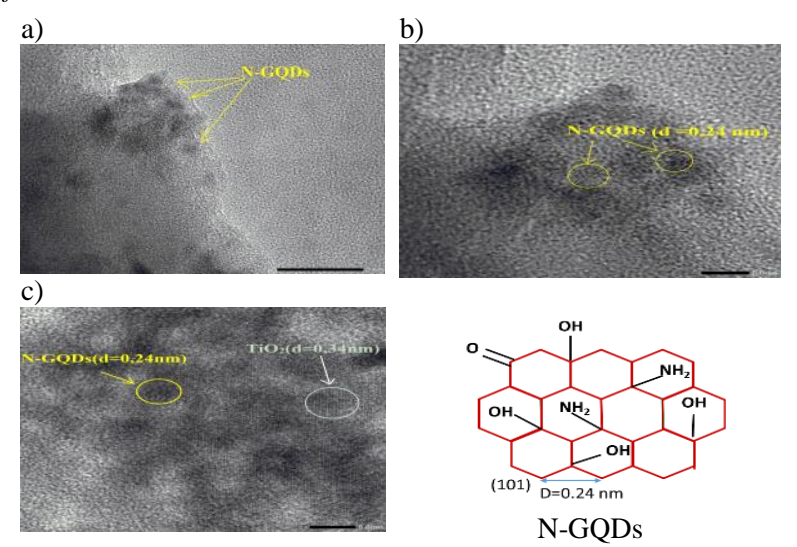


Figure 3.26. HRTEM image of (a) N-GQDs and (b) N-GQDs/TiO₂

f) XPS spectra of N-GQDs modified TiO₂

The blue shift of the Ti 2p peak can be attributed to a decrease in electron density around the titanium nuclei, resulting from a more negatively charged environment. The surface of nitrogen-doped graphene quantum dots contains various oxygen functional groups, contributing to this negative charge. Additionally, high-resolution X-ray photoelectron spectroscopy of the N 1s region reveals only one signal, which is characteristic of the amine groups (N-H) present in N-GQDs.

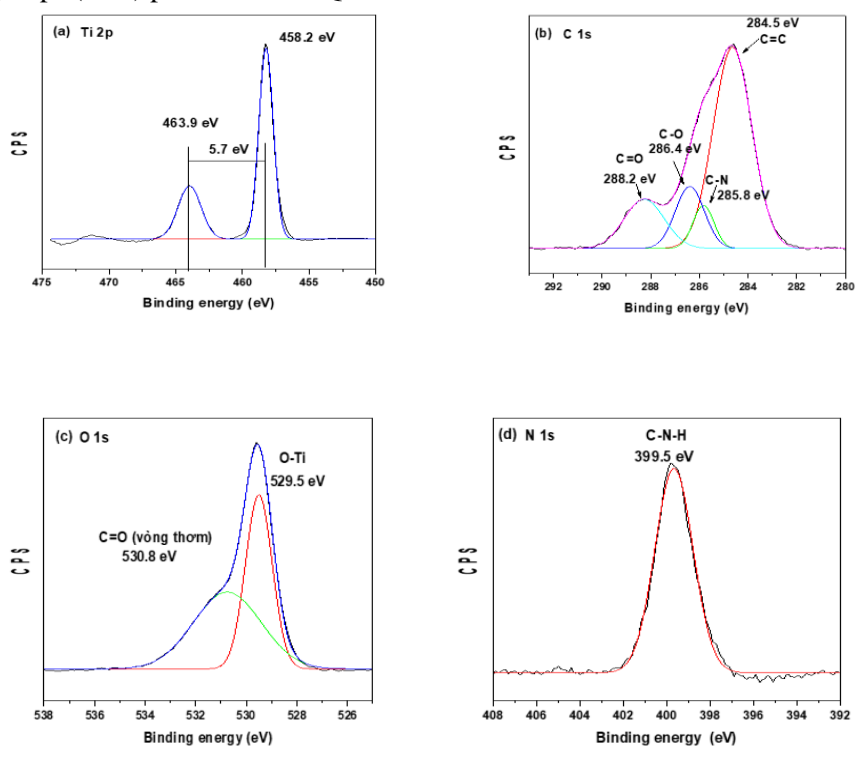


Figure 3.27. XPS spectra (a) Ti 2p, (b) C 1s, (c) O 1s and (d) N 1s of N-GQDs/TiO₂

3.1.3.2. Photocatalytic activity of N-GQDs modified TiO₂

The TiO₂ material adsorbs 35.29% of the MB concentration. The MB adsorption percentages for 1%-NGT, 5%-NGT, 10%-NGT, and 15%-NGT

are higher than those of TiO_2 , by 11.7%, 16.69%, 19.84%, and 19.43%, respectively. The adsorption mechanism for the interaction between N-GQDs/ TiO_2 and methylene blue is illustrated in Figure 3.30.

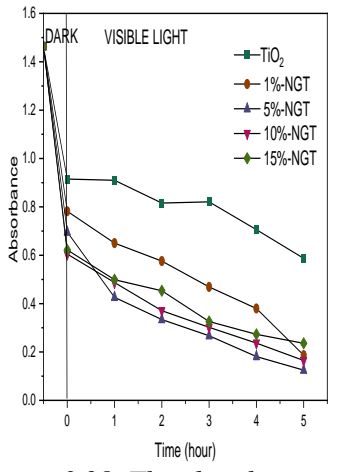


Figure 3.28. The absorbance of MB degradation under white light irradiation of TiO₂ and N-GQDs/TiO₂

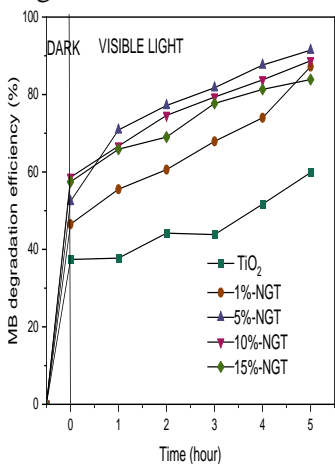


Figure 3.30. The MB decomposition efficiency of TiO₂ and N-GODs/TiO₂

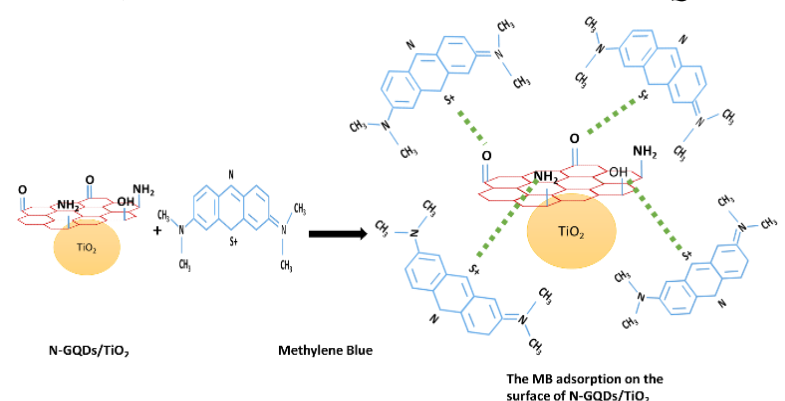


Figure 3.31. The adsorption interaction between N-GQDs/TiO₂ and methylene blue

The photocatalytic properties of pure TiO₂ and TiO₂ modified with nitrogen-doped graphene quantum dots in the visible region are better described by second-order kinetics. The 5% N-GQD modified TiO₂

exhibits the highest photocatalytic capacity, with a rate constant of 1.3 L/mol·hour, which is six times higher than that of pristine TiO₂.

3.1.4. Ag, N-GQDs modified TiO₂

3.1.4.1. Characteristics of Ag, N-GQDs/TiO₂

a) XRD pattern of Ag, N-GQDs/TiO2

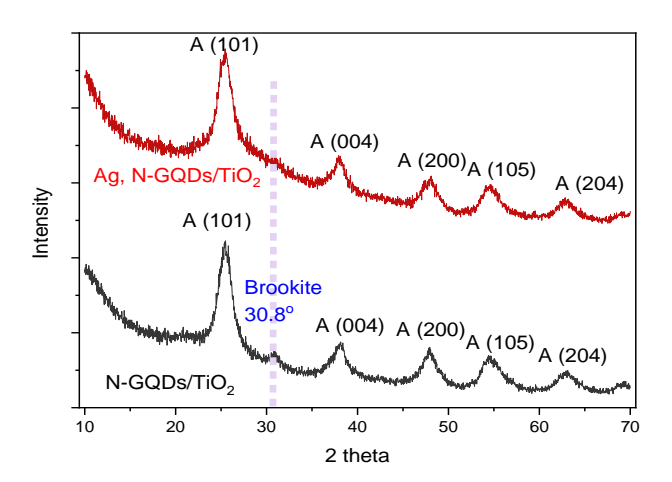


Figure 3.33. XRD pattern of N-GQDs/TiO2 and Ag, N-GQDs/TiO2

The size of the crystals can be determined using the Scherrer equation along with the collected data, as illustrated in Table 3.9.

Table 3.9. The crystal sizes of N-GQDs/TiO₂ and Ag, N-GQDs/TiO₂ were analyzed using XRD

Paremeter	N-GQDs/TiO ₂	Ag, N-GQDs/TiO ₂
Peak (2theta)	25.3	25.3
FWHM (theta)	0.725	0.8
FWHM (radian)	0.012654	0.013963
Crystal size (nm)	11.24	10.19

c) $UV-Vis\ spectra\ of\ Ag,\ N-GQDs/TiO_2$

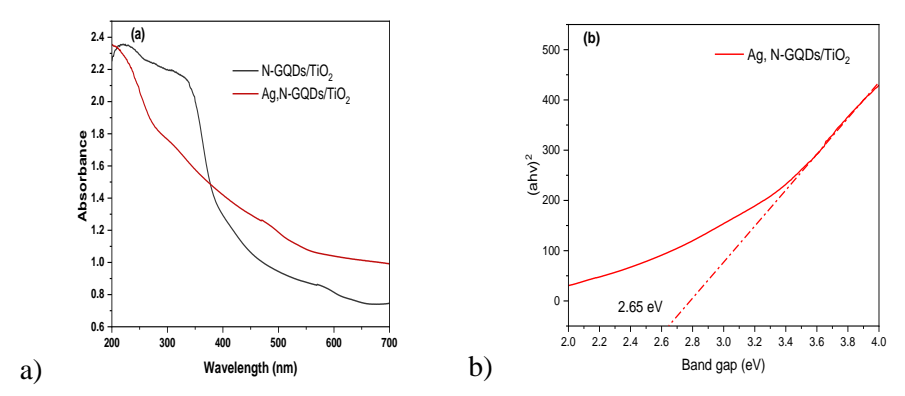
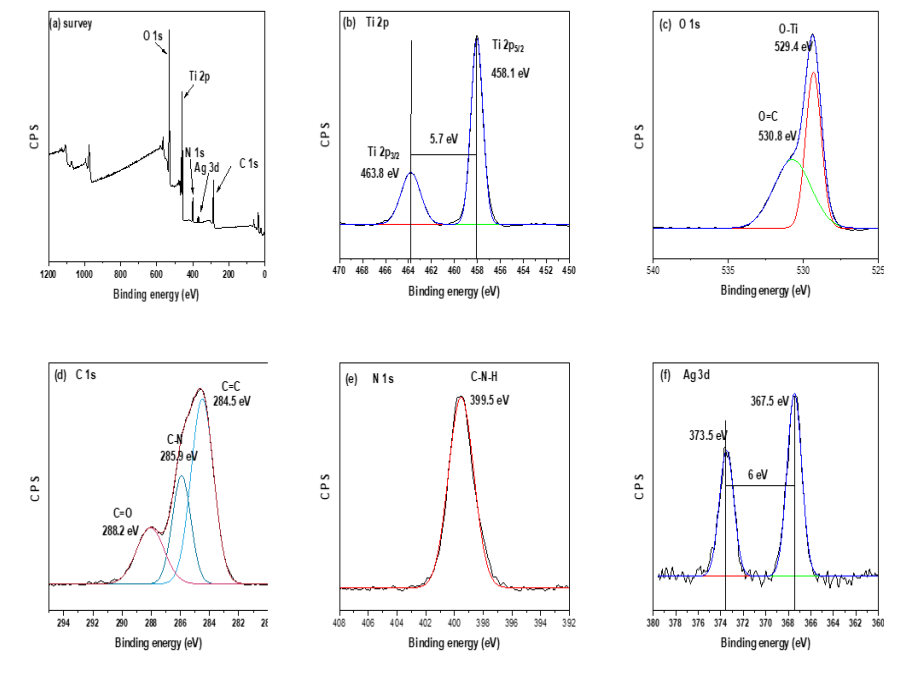


Figure 3.35. (a) UV-Vis and (b) Tauc plot of Ag, N-GQDs/TiO $_2$ f) XPS spectra of Ag, N-GQDs/TiO $_2$

Figure 3.39. XPS spectra of Ag, N-GQDs/TiO₂



The disappearance of O-H functional groups in the O 1s spectrum, along with the decreased intensity of the C-O peak in the C 1s spectrum,

indicates that C-O-H functional groups may be involved in the reduction process of Ag^+ ions.

3.1.4.2. Photocatalytic activity of Ag, N-GQDs/TiO₂

Regarding the photocatalytic activity of Ag, N-GQDs/TiO₂, the degradation of MB in the visible region was analyzed. The reaction kinetics for TiO₂, N-GQDs/TiO₂, and Ag, N-GQDs/TiO₂ best fit the pseudo-second-order model. Among these, Ag, N-GQDs/TiO₂ achieved the maximum rate constant (k = 2.1129 L/mol·hour), which is ten times greater than that of pure TiO₂ and three times greater than that of N-GQDs/TiO₂.

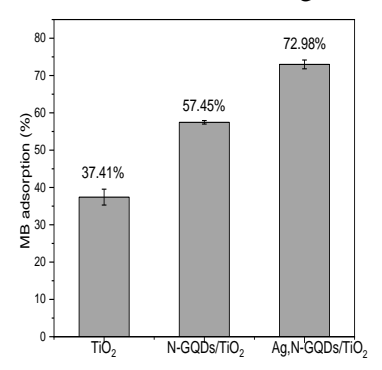


Figure 3.41. The MB absorption yield of TiO₂, N-GQDs/TiO₂, and Ag, N-GQDs/TiO₂

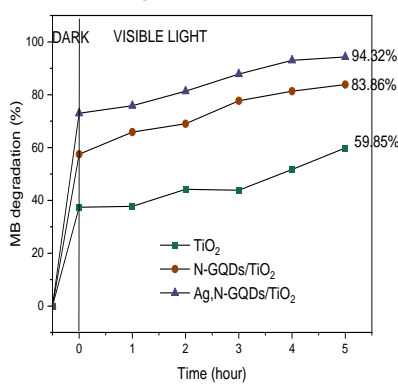


Figure 3.42. The MB degradation efficiency over time of TiO₂, N-GQDs/TiO₂, and Ag, N-GQDs/TiO₂

Table 3.10. The rate constant of the MB degradation reaction under visible light irradiation of TiO₂, N-GQDs/TiO₂, and Ag, N-GQDs/TiO₂

	First pseudo-kinetic		Second pseudo-		
Material			kinetic		
	\mathbb{R}^2	k	\mathbb{R}^2	k	
TiO ₂	0.86241	0.1972	0.90279	0.20232	
N-GQDs/TiO ₂	0.88021	0.43184	0.9615	0.74909	
Ag,N-GQDs/TiO ₂	0.90032	0.65616	0.96834	2.1129	

3.2. Research results on the characteristics and photocatalytic activity of Ag, N-GQDs/ZnO $\,$

3.2.1. Zinc Oxide

3.2.1.1. Characteristics of ZnO *a) XRD of ZnO*

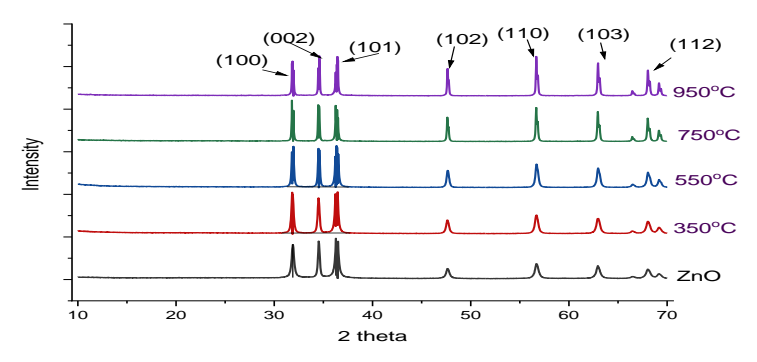


Figure 3.44. XRD pattern of ZnO

The wurtzite structure is the preferred formation of ZnO, which is synthesized using the sol-gel method with water as the solvent at room temperature or when calcined at temperatures below 950 °C under atmospheric pressure. Additionally, the crystal lattice size of ZnO produced by this method is minimally influenced by temperature changes.

3.2.1.2. Photocatalytic activity of ZnO

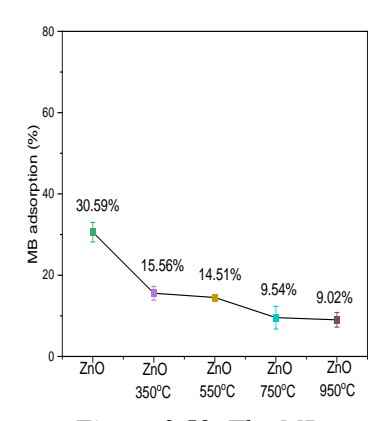


Figure 3.52. The MB adsorption efficiency of ZnO

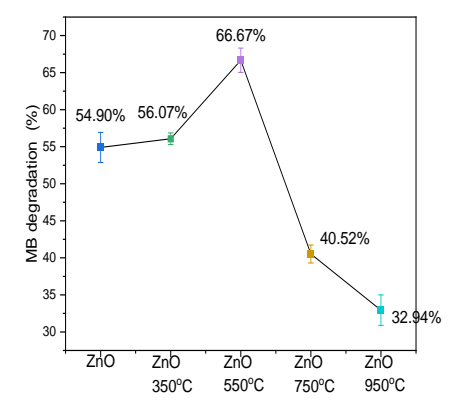


Figure 3.53. The MB degradation yield of ZnO after 50 mins UV irradiation

The MB degradation process under UV light is better described by the first pseudo kinetic model (2.11). The ZnO calcined at 550 $^{\circ}$ C demonstrates the best capability for MB degradation (k = 0.01696 min⁻¹).

3.2.2. Ag modified ZnO

3.2.2.1. Characteristics of ZnO

d) EDX spectra of Ag modified ZnO

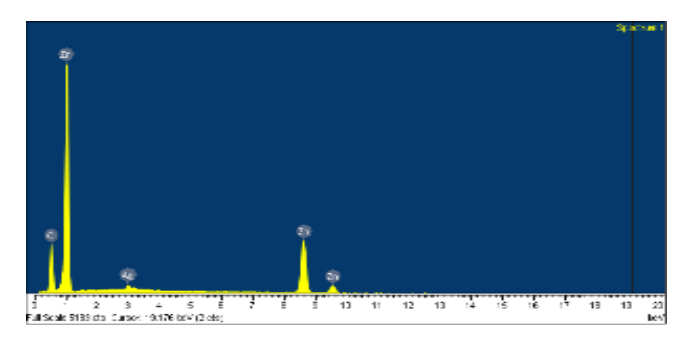


Figure 3.59. EDX spectra of Ag1%/ZnO

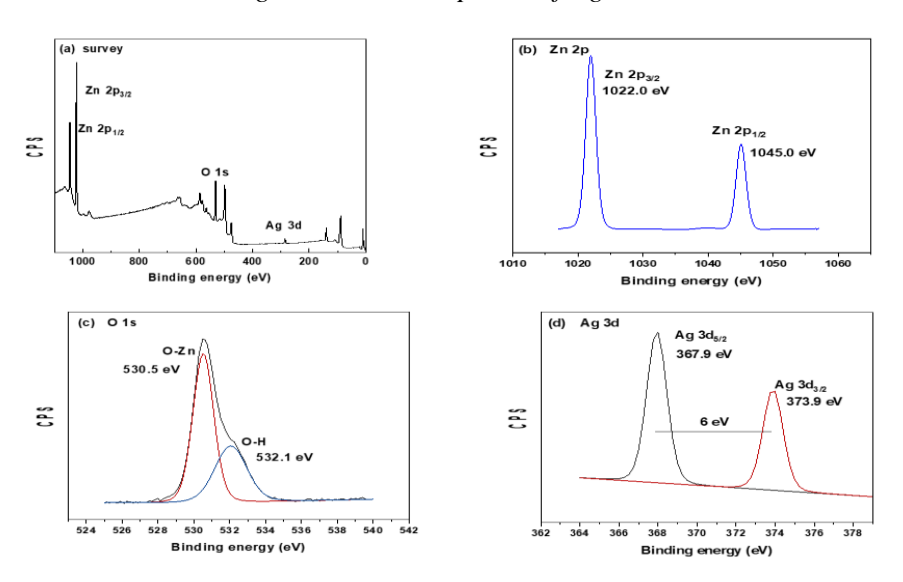


Figure 3.60. XPS spectra of Ag1%/ZnO (a) survey, (b) Zn 2p. (c) O 1s, and (d) Ag 3d

e) XPS spectra of Ag modified ZnO

The XPS survey shown in Figure 3.60a reveals signals for Zn 2p, O 1s, and Ag 3d. The high-resolution XPS spectra for Ag 3d (Figure 3.60d) display two distinct peaks at 367.9 eV and 393.9 eV, which correspond to the Ag 3d_{5/2} and Ag 3d_{3/2} levels, respectively. The binding energy difference between these peaks remains consistent at 6 eV. Notably, there is no additional peak for Ag⁺, indicating that silver is present in its metallic form.

3.2.2.2. Photocatalytic activity of Ag modified ZnO

a. Photocatalytic activity of Ag/ZnO for MB degradation

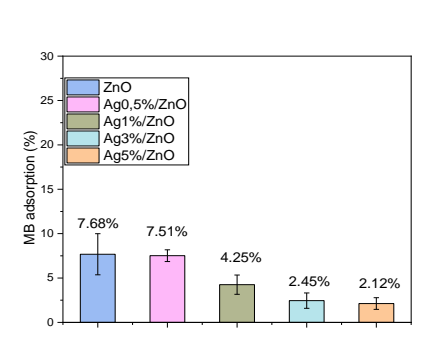


Figure 3.62. The MB adsorption efficiency after 30 minutes in the dark

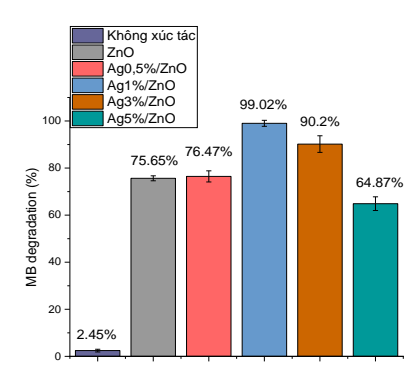
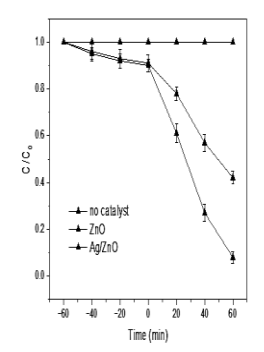
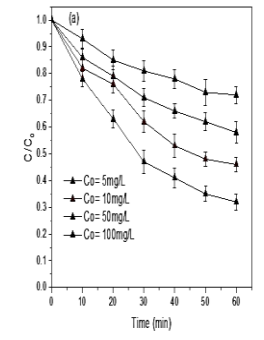


Figure 3.63. The MB degradation efficiency after 50 minutes under UV irradiation

b. Photocatalytic activity of Ag/ZnO for caffeine degradation





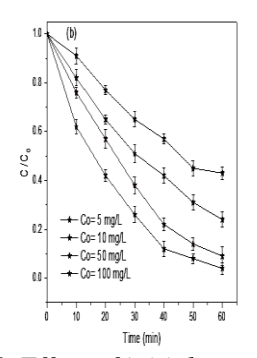


Figure 3.64. Photodegradation of caffeine using different catalysts

Figure 3.65. Effect of initial concentration on degradation of caffeine using (a) ZnO và (b) Ag/ZnO

The proposed mechanism of caffeine degradation using Ag/ZnO catalyst under sunlight irradiation is as follows:

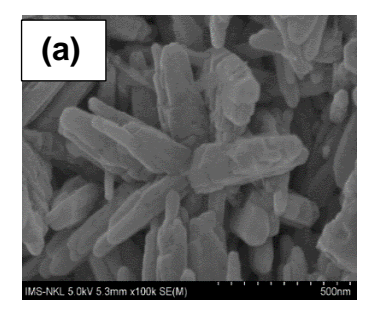
Ag/ZnO + hv
$$\rightarrow$$
 Ag/ZnO (e⁻ + h⁺)
e⁻ + O₂ \rightarrow O₂⁻
h⁺ + H₂O \rightarrow OH $^{\bullet}$ + H⁺
OH $^{\bullet}$, O₂⁻ + caffeine \rightarrow H₂O + CO₂ + by products

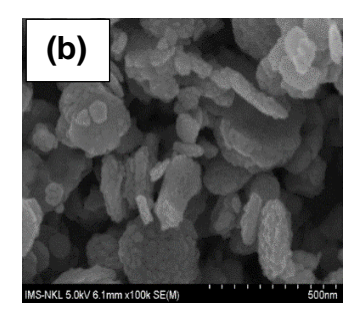
The stability of the Ag/ZnO photocatalyst was evaluated over eight testing cycles. The Ag/ZnO demonstrated a remarkable photodegradation capacity for caffeine, achieving 78.6% degradation after five cycles. However, this effectiveness declined to 48.2% by the eighth cycle.

3.2.3. Ag, N-GQDs/ZnO

3.2.3.1. Characteristics of Ag, N-GQDs/ZnO

c) SEM image of Ag, N-GQDs/ZnO





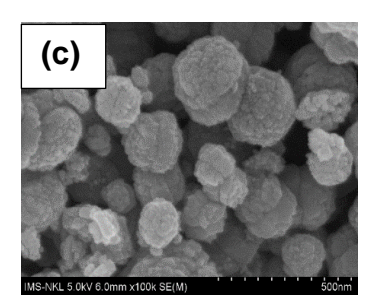
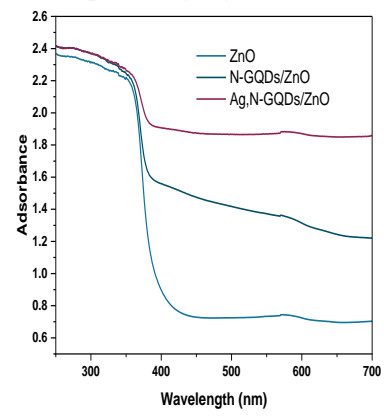


Figure 3.71. SEM image of (a) ZnO, (b) N-GQDs/ZnO, (c) Ag, N-GQDs/ZnO

The N-GQDs dots act as a capping agent that will change the shape of the forming material. The N-GQDs/ZnO material has a plate-like structure, with a nanometer thickness of about 25 nm - 50 nm.

d) UV-Vis spectra of Ag, N-GQDs/ZnO



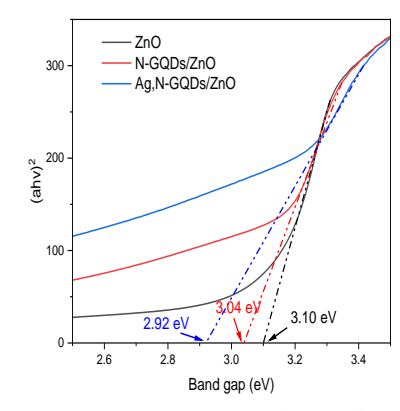


Figure 3.72. UV-Vis spectra of ZnO, N-GQDs/ZnO, and Ag, N-GQDs/ZnO

Figure 3.73. Tauc plot and band gap of ZnO, N-GQDs/ZnO, and Ag, N-GQDs/ZnO

The band gap energies for ZnO, N-GQDs/ZnO, and Ag, N-GQDs/ZnO are 3.10 eV, 3.04 eV, and 2.92 eV, respectively (Figure 3.73). The simultaneous combination of noble metal and carbon nanomaterials with ZnO can reduce the band gap energy to a level lower than that of pure ZnO and the N-GQDs/ZnO hybrid material.

d) Energy dispersive X-ray spectrum of Ag, N-GQDs/ZnO materials

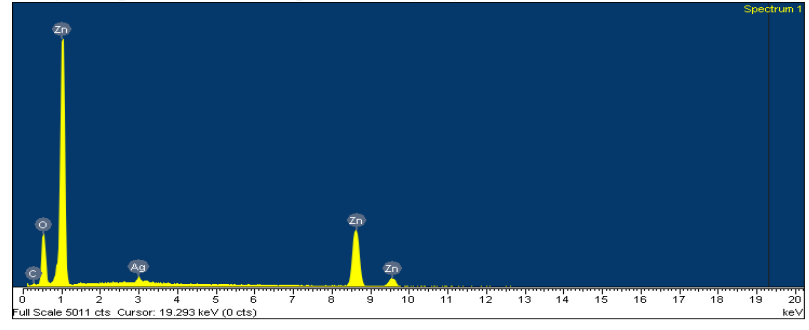


Figure 3.75. EDX image of Ag, N-GQDs/ZnO

3.2.3.2. Photocatalytic activity of Ag, N-GQDs/ZnO

Table 3.20. Rate constant values of the MB degradation reaction under visible light of ZnO, N-GQDs/ZnO, and Ag, N-GQDs/ZnO

	First pseu	ıdo-kinetic	Second pseudo-kinetic		
Material	Coefficient R ²	Rate	Coefficient R ²	Rate	
Material		constant - k		constant - k	
		(hour ⁻¹)		(L/mol.hour)	
ZnO	0.8229	0.12314	0.84694	0.20436	
N-GQDs/ZnO	0.79864	0.20415	0.83689	0.39996	
Ag, N- GQDs/ZnO	0.76903	0.20415	0.81386	0.69519	

Modifying ZnO with graphene quantum dots (N-GQDs) and noble metal nanoparticles like silver (Ag) will enhance the photocatalytic capability of this material in the visible region by up to 3.5 times.

CONCLUSION

During the research and development of photocatalytic materials based on TiO_2 and ZnO, which were modified with nitrogen-doped graphene quantum dots and Ag nanoparticles, the following results were obtained:

1. The materials TiO₂ and ZnO were successfully fabricated using the sol-gel method, followed by high-temperature calcination. TiO₂ undergoes a phase transformation, with the rutile phase emerging at calcination temperatures above 650 °C. All the fabricated TiO₂ materials are capable of decomposing organic dyes when exposed to ultraviolet (UV) light. Specifically, the TiO₂ material calcined at 450 °C exhibits the highest effectiveness in decomposing methylene blue (MB) and rhodamine B (RhB) in the UV range, achieving decomposition rates of 88.76% and 50.05%, respectively. This material has a mixed structure, consisting of approximately 88.6% anatase and 11.34% brookite, with a spherical shape and an average size of about 20 nm. Conversely, the ZnO material calcined at 550 °C demonstrates the highest efficiency in decomposing MB under UV light, achieving a decomposition rate of 66.67%. This ZnO possesses a wurtzite crystal structure, a spherical shape, and a low bandgap energy of approximately 3.06 eV. On the other hand, the uncalcined ZnO material

features a long rod shape but shares the same bandgap energy of 3.06 eV. It exhibits a superior ability to absorb visible light, making it advantageous for photocatalysis in the visible range.

- 2. Silver-modified TiO₂ and ZnO were fabricated using a chemical reduction method combined with UV irradiation. The Ag/TiO₂ materials, with silver content ranging from 0.1% to 0.5%, demonstrated a superior ability to decompose methylene blue (MB) in the UV region compared to pure TiO₂. Silver acts as an electron trap, which increases the average lifetime of the electron-hole pairs from 42.12 ps to 77.51 ns. For ZnO surface modification, the most appropriate silver content was found to be 1%, resulting in a band gap energy of 2.93 eV. The Ag/ZnO material was able to decompose 99.02% of MB under UV light and 97.20% of caffeine using sunlight. After five reuse cycles, Ag/ZnO decomposed 78.6% of caffeine, with superoxide (O₂··) identified as the primary agent responsible for caffeine decomposition in aqueous environments.
- 3. A simple mixing method was successfully used to fabricate N-GQDs/TiO2 and N-GQDs/ZnO materials. The N-GQDs (nitrogen-doped graphene quantum dots) measured approximately 5 nm in size and featured oxygen-containing functional groups on their surfaces, which enhanced their ability to adsorb methylene blue (MB). In the visible region, the N-GQDs/TiO₂ composite with 5% N-GQDs decomposed methylene blue (91.45%), compared to TiO₂ alone (59.85%), achieving a reaction rate constant of 1.29838 l/mol·hour. The MB decomposition reaction rate N-GODs/ZnO material constant for the is 0.39996 1/mol·hour. Additionally, the band gap energy of N-GQDs/TiO2 is 3.02 eV, while that of N-GQDs/ZnO is 3.04 eV.
- 4. The study successfully developed multilayer photocatalytic materials, Ag, N-GQDs/TiO2 and Ag,N-GQDs/ZnO, using a chemical reduction method. Hydroxyl (-OH) functional groups on the surface of N-GQDs acted as direct reductants, converting Ag⁺ ions into metallic Ag nanoparticles. The integration of these components significantly enhanced light-harvesting capabilities, leading to a reduction in the band gap to 2.65 eV for Ag, N-GQDs/TiO₂ and 2.92 eV for Ag, N-GQDs/ZnO.

In terms of mechanism, N-GQDs functioned as effective photosensors while Ag nanoparticles provided an electron trapping effect, which reduced the recombination of electrons (e⁻) and holes (h⁺). Consequently, these materials demonstrated exceptional methylene blue (MB) degradation efficiencies under strong light illumination, achieving rates of 94.23% and 68.37% degradation, with continuous reaction rates of 2.1129 L/mol·hour and 0.69519 L/mol·hour, respectively.

RECOMENDATION

The thesis has presented a scientific foundation and the synthesis process for a new generation of photocatalytic materials that function efficiently in the visible light spectrum. This is achieved by combining traditional TiO_2 and ZnO with precious metal nanoparticles, specifically silver (Ag), and nitrogen-doped graphene quantum dots. The research findings indicate that these new materials demonstrate a superior ability to photodegrade organic compounds in the visible region. This capability allows them to replace catalysts that only work under UV light, thus optimizing the utilization of natural sunlight to treat dissolved pollutants in water. However, due to time and resource constraints during the thesis implementation, it is recommended to continue exploring the following areas:

It is essential to continue studying the visible light photocatalytic abilities of Ag, N-GQDs/TiO₂, and Ag, N-GQDs/ZnO materials in real wastewater. Additionally, we need to evaluate the factors that affect the photocatalytic performance of these materials.

Furthermore, it is important to design an optimized reactor system to enhance the wastewater treatment process using Ag, N-GQDs/TiO₂ and Ag, N-GQDs/ZnO photocatalytic materials.

LIST OF THE PUBLICATIONS RELATED TO THE DISSERTATION

1. Minh Thuy Pham, Thi Thu Hien Chu, Duc Chinh Vu, "Mitigation of caffeine micropollutants in wastewater through Ag-doped ZnO photocatalyst: mechanism and environmental impacts", Environ Geochem Health (2024) 46:168 https://doi.org//s10653-024-01952-1

2. Minh Thuy Pham, Duc Chinh Vu, Thi Thu Hien Chu, Thuy Van Nguyen, "Multi-timescale map of radiative and nonradiative decay for exciton in Ag/TiO₂ nanoparticles" Optical Materials /159 (2025) 116607

https://doi.org/10.1016/j.optmat.2024.116607